Rotating annulus experiment: Large-scale helical soliton in the atmosphere?

Zhao Songnian,[1] Xiong Xiaoyun,[2] Hu Fei,[1] and Zhu Jiang[1]
[1]*State Key Laboratory of Atmospheric Boundary Layer Physics and Atmospheric Chemistry, Institute of Atmospheric Physics, Chinese Academy of Sciences, Beijing 100029, China*
[2]*Commission of National Natural Science Foundation of China, Beijing 100085, China*
(Received 4 December 2000; revised manuscript received 15 March 2001; published 29 October 2001)

A typhoon is a cyclone vortex with a warm low pressure center, formed over tropical oceanic waters. A large-scale rotating annulus experiment of fluid dynamics is carried out, under the conditions of dynamic similarity, geometric similarity, and the similarity of boundary conditions. In the first step, with the help of infrared heaters, the basic flow field and helical structure of a single typhoon were successfully simulated; then two model typhoons were generated, and their interactions tested. It demonstrated that they did separate after colliding with each other, and their respective basic shapes were restored, which confirms the basic dynamic features of typhoons in nature as solitons. It was also shown that the formation of their helical structures is related to the adapting process of atmosphere to the rotation of the earth and that their dynamic characteristics as solitons come from a result of an equilibrium between their dispersion and the nonlinear convergence of the anticyclones, with whose combined actions their structure remains stable for a long period, which in turn means that they are indeed three-dimensional helical solitons.

DOI: 10.1103/PhysRevE.64.056621 PACS number(s): 05.45.Yv, 92.60.Qx, 47.32.Cc

I. INTRODUCTION

Formed over tropical oceans, a typhoon is a three-dimensional cyclone vortex having a warm low pressure center. Meteorologists have observed and studied typhoons for a long time [1–3], with their research focuses on the mechanism of their development and predictions of their motion [4–6]. Along with numerical calculations, the rotating annulus experiment remains to be an important method for studying the dynamic characteristics of a large-scale rotating fluid [7–10]. A typhoon acquires a helical structure under the action of Coriolis force due to the rotation of the earth. From the view point of nonlinear dynamics, a typhoon is mainly affected by the following three factors: advection, dissipation, and dispersion. Advection, as a nonlinear action, leads to a very steep convex wave shape. Dispersion tends to expand the wave shape wider and the dissipation will attenuate the wave amplitude. These conflicting factors, when approaching to an equilibrium state, drive a typhoon forward with stable helical structure and a constant speed for a long time. These characteristics are similar to those of a soliton. In addition, barotropic vortex equations for rotating atmosphere and the wave equations at a low latitude can both be reduced to the KdV equations in the first-order approximation [11,12]. Makino, Kamimura, and Taniuli [13] have conducted numerical experiments for two colliding vortexes according to the above mentioned dynamic features of a soliton. The two vortexes, after colliding with each other, have separated and restored their respective wave shapes and traveling speeds, which proves this kind of vortexes behave like two-dimensional solitons in nature. All these lead us to believe that a typhoon may be a helical soliton created by nature. In order to confirm this idea, we have conducted a series of large-scale fluid dynamic rotating annulus experiments, which have fairly well modeled the macroscopic dynamic features of typhoon in nature such as its large-scale helical structure and basic flow field. In these dynamic experiments, it is found that two different model typhoons, after colliding with each other, will separate and restore their respective basic structures. Our experimental results demonstrated that a typhoon possesses the main dynamic characteristics of a soliton with a rather stable helical structure. Therefore, it may be said that a typhoon is a large-scale helical soliton. This finding also suggested that the nonlinear theory of the solitary wave provides a new approach to the study of typhoons and is helpful in understanding the formation mechanism and dynamic characteristics of typhoons.

II. THE MATHEMATICAL AND PHYSICAL BACKGROUND OF THE MODEL

A. The basic structure of the model typhoon

A typhoon is a three-dimensional low pressure cyclone vortex with a ratio of vertical and azimuthal scales of about 1:50. It has nearly axially symmetric distributions of air pressure, temperature, and wind field. Its vortex radius typically ranges from 500 to 1000 km. It is convenient to describe a typhoon according to its three zones. The outer zone consists of helical cloud bands. The middle zone is a ring with the maximum wind speed strong convection, and rainfall. The central zone is the so-called eye of the typhoon formed by ring shaped cloud walls, measuring about 10 to 70 km across, where winds are weak. It is very dry, warm, and nearly free of clouds in the eye. The typhoon rotates around a vertical axis with a great speed, developing into a strong vertical air flow towards the middle layer with the air entering from the lower layer, where the tangential wind component is dominant and radial component is small. The air on the top layer then flows out and mixes with surrounding air, sinking down to form a radial-vertical circulating ring. The vertical height of a typhoon ranges from 10 to 20 km. At a height of 100 to 150 km from the eye is the anticyclone circulating air flow, which sucks out the air, resulting in a

TABLE I. Seven nondimensional parameters as independent similarity criteria for experiment modeling and comparison of their experimental value and actual observational value.

Parameter	Formula	Range of experimental value	Range of actual observational value
Rossby number	$\mathrm{Ro}=U/LF$	$\mathrm{Ro}_e=0.32-0.43$	$\mathrm{Ro}_n=0.6-1.6$
Ekman number	$\mathrm{Ek}=\nu/fL^2$	$\mathrm{Ek}_e=2.5\times10^{-4}-0.79\times10^{-4}$	$\mathrm{Ek}_n=0.4\times10^{-4}-1.7\times10^{-3}$
Prandtl number	$\mathrm{Pr}=\upsilon/k$	$\mathrm{Pr}_e\approx1$	$\mathrm{Pr}_n\approx1$
Froude number	$\mathrm{Fr}=U^2/gL$	$\mathrm{Fr}_e=0.25\times10^{-4}-3.0\times10^{-4}$	$\mathrm{Fr}_n=0.9\times10^{-4}-3.2\times10^{-4}$
Time parameter	$H_0=tU/L$	$H_{0e}=(1.35-1.5)\times10$	$H_{0n}=(1.04-1.56)\times10$
Storm development law	$D=\dot{Q}L/C_pTU$	$D_e=(1.3-2.0)\times10^{-1}$	$D_n=(0.9-1.2)\times10^{-1}$
Geometric parameter	$G=H/L$	$G_e=0.025-0.030$	$G_n\approx0.02-0.03$

very low pressure at the center of the typhoon. The model typhoon in the rotating annulus experiment at laboratory should have all those basic flow structures as the actual typhoon in nature.

B. Experimental model

According to a theory called conditional instability of the second kind, release of latent heat from moisture condensation, serving as a positive feedback in heating the atmosphere, plays a key role in the formation of typhoons [14,15]. Anthes [2] and Yamasaki [16] proposed a mathematical model to describe this process, whose original equations in cylindrical coordinates are essentially Navier-Stokes equations with Coriolis force included, that are

$$\frac{\partial \nu_\lambda}{\partial t}+\nu_r\frac{\partial \nu_\lambda}{\partial r}+\frac{\nu_\lambda}{r}\frac{\partial \nu_\lambda}{\partial \lambda}+w\frac{\partial \nu_\lambda}{\partial z}+f\nu_r+\frac{\nu_\lambda\nu_r}{r}=\frac{1}{\rho r}\frac{\partial p}{\partial \lambda}+\frac{1}{\rho}\frac{\partial \tau_{z\lambda}}{\partial z}+\frac{1}{\rho}\left(\frac{\partial \tau_{r\lambda}}{\partial r}+\frac{\partial \tau_{\lambda\lambda}}{r\partial\lambda}+\frac{\tau_{r\lambda}-\tau_{\lambda\lambda}}{r}\right), \quad (1)$$

$$\frac{\partial \nu_r}{\partial t}+\nu_r\frac{\partial \nu_r}{\partial r}+\frac{\nu_r}{r}\frac{\partial \nu_r}{\partial \lambda}+w\frac{\partial \nu_r}{\partial z}-f\nu_\lambda-\frac{\nu_\lambda^2}{r}=-\frac{1}{\rho r}\frac{\partial \rho}{\partial \lambda}+\frac{1}{\rho}\frac{\partial \tau_{zr}}{\partial z}-\frac{1}{\rho}\left(\frac{\partial \tau_{rr}}{\partial r}+\frac{1}{r}\frac{\partial \tau_{\lambda r}}{\partial \lambda}+\frac{r_{rr}-\tau_{r\lambda}}{r}\right), \quad (2)$$

where ν_r and ν_λ represent the radial and tangential components of the velocity, respectively, and τ is the vortex stress. The following equations should be added for numerical calculations.

Equation of statics,

$$\frac{\partial p}{\partial z}=-pg, \quad (3)$$

continuity equation,

$$\frac{\partial \rho}{\partial t}+\frac{\partial \rho\nu_\lambda}{r\partial\lambda}+\frac{\partial \rho r\nu_r}{r\partial\lambda}+\frac{\partial \rho w}{\partial z}=0, \quad (4)$$

equation of state,

$$p=\rho RT, \quad (5)$$

equation of thermodynamics,

$$\frac{d\theta}{dt}=\frac{0}{C_pT}\dot{Q}+\frac{1}{r}\frac{\partial}{\partial r}\left(rK_H\frac{\partial\theta}{\partial r}\right)+\frac{\partial}{\partial z}\left(K_Z\frac{\partial\theta}{\partial z}\right)+\frac{1}{r^2}\frac{\partial}{\partial\lambda}\left(K_H\frac{\partial\theta}{\partial\lambda}\right), \quad (6)$$

equation of water balance,

$$\frac{dq}{dt}+p-E+S=\frac{1}{r}\frac{\partial}{\partial r}\left(rK_H\frac{dq}{d\lambda}\right)+\frac{\partial}{\partial z}\left(K_Z\frac{\partial q}{\partial z}\right)+\frac{1}{r^2}\frac{\partial}{\partial\lambda}\left(K_H\frac{\partial q}{\partial\lambda}\right), \quad (7)$$

expression for potential temperature,

$$\theta=T\left(\frac{P_0}{P}\right)^{R/C_p}, \quad (8)$$

where θ is the potential temperature, ρ the density, K_H and K_Z are horizontal and vertical eddy viscosity coefficients, respectively, p is the air pressure, E is the vapor, S is the liquid water in the air, and $\dot{Q}$ is the nonadiabatic heating rate.

The solutions of these equations, after scale analyses and simplifications, lead to a set of nondimensional parameters, as shown in Table I of the following section which may serve as the basis for the design of experiment modeling and related interpretations.

C. Similarity criteria for experiment modeling

The large-scale fluid dynamic rotating annulus is designed based on the mode of the geostrophic motion. In order to simulate the large-scale helical motion in the nature governed by relevant Eqs. (1)–(8), the experimental conditions should be such that the dynamic similarity, the geometric similarity, and the similarity in boundary conditions are maintained. From this seven independent similarity criteria can be derived [17,18] as shown in Table I, where subscript

e represents values used in the experimental setup and subscript *n* indicates the actual observational values. As the actual observational values for U, L, and $\dot{Q}$ are only the averaged estimations, there are some differences between the related nondimensional quantities and the experimental ones. But their actual effects are limited, for a model typhoon the basic requirements of Rossby number Ro, <1 and Ekman number Ek $\ll 1$ are satisfied automatically.

From Table I, it can be seen that the dynamic and thermodynamic constraints are satisfied in our experiments, which means that the experiment conforms rigorously with the theory of similarity, therefore, it will simulate not only the general features of a typhoon, but also its important structures, such as the temperature field, flow field, and the eye region. The results of the experiment indeed agree with the actual observation data and basic facts in meteorology, so the simulation of the dynamic process for the interaction of two typhoons is based on a solid foundation of mathematics and physics.

In our experiment the air is used as the working media, so the value for the gas law $A_s = pRT$ is equal to 1; and H the height, L the horizontal scale, U the horizontal speed, T the temperature, R the gas constant, C_p the specific heat capacity at constant pressure, $\dot{Q}$ the nonadiabatic heating rate, p the air pressure, ρ the air density, ν the eddy viscosity coefficient, t the time, f the Coriolis parameter, and k the heat transfer coefficient.

Note that the H_0, D and G are also important similarity indices. We summarize their dynamic meanings as follows.

(1) The dynamic meaning of H, harmony-time parameter is that the dynamic process of a natural typhoon should be similar to one of the model typhoons. In other words, the H_{0e} and H_{0n} are of the same order of magnitude. For a natural typhoon the time required from initial disturbance to its mature state is about 3 days, i.e., $t_n = 3d$ and $U_n = 30-40$ ms, $L_n = 500-1000$ km. Using the formula $H_0 = t_n U_n / L_n$, we have $H_{0n} = 10(1.56-1.04)$, for the model typhoon. $U_e = 3-4$ m/s, $L_n = (30-40)$ m, $t_r = 4-5$ rotation period (namely, 4–5 disk days), and the rotation period is in the range of 30–45 s. Then we have $H_{0e} = 10(1.35-1.5)$.

(2) Storm development law D indicates the degree of development of typhoon or tropical cyclone. $\dot{Q}_n$ is the condensing heating rate that comes from the strong mesoscale cumulus tower surrounded the typhoon's eye. We assume its vapor convergence is about 40 g/cmd, therefore, $\dot{Q}_n = 2.0 \times 10$ J/g s. For the model typhoon, the infrared light bulb used in the experiment is 12 W in electric power, of which 1–1.2 W can be converted to infrared radiation energy, only 0.2–0.3 W of which is absorbed by cigarette smoke. Therefore, we can calculate the value of $\dot{Q}_e$, that is 2.7 J/g s. When the values of U_e, L_e, and U_n, L_n are the same as in Eq. (1), we have $D_e = (1.3-2.0) \times 10^{-1}$ and $D_n = (0.9-1.2) \times 10^{-1}$, respectively.

(3) Geometric parameter G is determined by the actual size of natural typhoons, from which we determine the size of rotating annulus and G of the model typhoon.

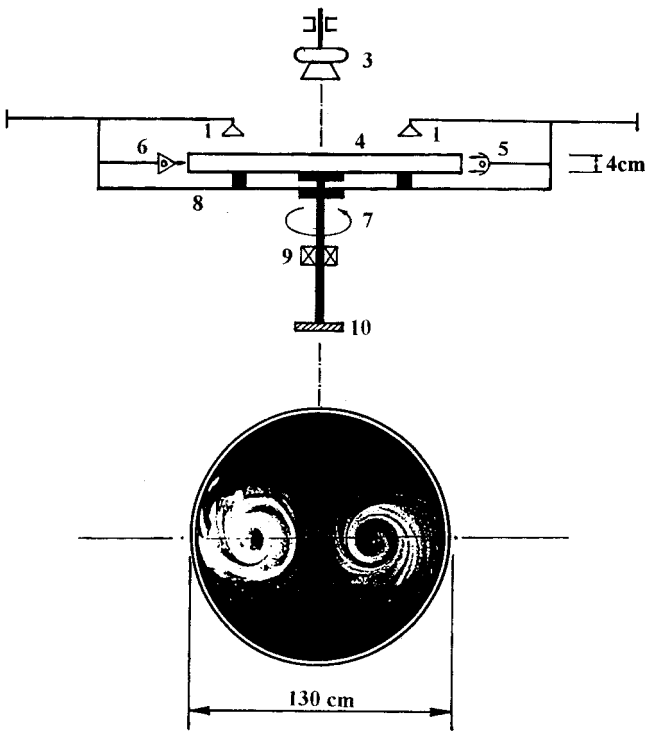

FIG. 1. Diagram of experimental setup. (1) Infrared heaters; (2) heating holes for infrared light; (3) high-speed camera; (4) gas vessel; (5) vertical sheet light source; (6) horizontal sheet light source; (7) axis to rotate horizontally; (8) horizontally rotating platform; (9) rotation controller; and (10) foundation.

III. EXPERIMENTAL SETUP

Our experimental setup is schematically shown in Fig. 1, where the gas vessel (4) is filled with air, used as the working media, two infrared heaters (1) heat the smoke entering the vessel through two small holes, and the overhead high speed camera (3) takes pictures of the experimental results. In order to observe more clearly the helical structures and the flow field of typhoons, some smoke (from burning cigarettes) is fed into the vessel by medical syringe needles through two special injecting holes at the side of the heating holes, which serves both as tracer gas for observing the atmospheric motion and the heat source for heating the surrounding air. The gas vessel is made of transparent plexiglass, in the shape of a cylinder, 130 cm in diameter, 4 cm in height. The platform (8), 350 cm in diameter, can rotate horizontally and is fixed with the gas vessel (4) with the same axis and with the rotation period of 20 through 180 s (continuously adjustable). The rotation period is an important control parameter in our experiments and takes values from 30 to 45 s, corresponding to rotating speeds of 0.21–0.14 rad/s. Within the above range, the L value of the model typhoon is 30–40 cm, and the H value is 3–3.6 cm. These values are chosen to make a full use of the space of the vessel in our experiments. The rotation period takes a value of 45 s in the experiment, that is, 0.14 rad/s and corresponds 24 h in the actual atmospheric process. Such a setup may provide enough space for the whole process of the interaction between two typhoons.

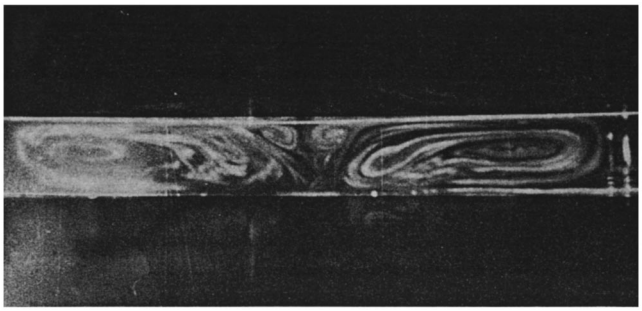

FIG. 2. Vertical structure of the model typhoons.

A. Infrared heaters

The infrared light bulbs required were chosen to be 12 W in power, according to the value of $\dot{Q}$ (see Sec. II C) and the actual absorption rate of infrared energy by the cigarette smoke. The absorption rate is calculated from the infrared absorption spectrum of the smoke. With the help of a focusing reflector, light beams of 1.8–2.0 cm in diameter will be formed. On the plexiglass plate over the gas vessel, is a central seam of $2\times120\,\mathrm{cm}^2$, which is closely sealed with a film that is well transparent to the infrared light. Through the seam the infrared radiation enters the gas vessel and is mostly absorbed by the smoke where the energy is stored to be used in heating the surrounding air in the later stage.

The smoke is injected into the gas vessel by medical syringe needles through the two special injecting holes near the heating seam. The injecting holes will be automatically sealed themselves as soon as the needles have been withdrawn, so the gas in the vessel will not leak out. The injected smoke has a very wide absorption spectrum band in the infrared region (with wavelength range of 2.5–6.3 μm). When being mixed with the surrounding air, the smoke will heat the air with the energy absorbed from infrared radiation and, at the same time, will clearly show the motion trajectories of the mixed air. Thus the basic flow field and helical structure of the formation of typhoons will be clearly visualized [17,18].

It must be pointed out that the heating process after the smoke is injected into the vessel goes side by side with the uniform counterclockwise rotation of the annulus at a prescribed speed. The heating process lasts about 3–4 min. each time (it is relevant with the scale of the model typhoon), and the characteristic scale of the model typhoon formed is in the range of 30–40 cm.

The intensity of infrared heater can be adjusted by varying the supply voltage. When the value of applied voltage is below 4 V the corresponding electrical power of heater is below 10 W. In such case the model typhoon cannot form in the time interval determined by the time similarity criterion H_0.

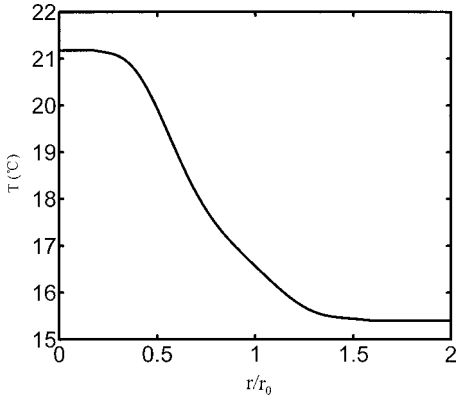

FIG. 3. Temperature distribution of a single typhoon in a vertical section.

B. Display and measurements

For the visualization observing and taking pictures of model typhoons, the vertical and horizontal light sheets that are about 0.6 cm thick (for the horizontal one) and have a power of 0.5 W, each are mounted on the platform. The light sheets are turned on only while taking pictures or during observation of the flow field in order to minimize interference with the experiment. The horizontal light sheet that is movable in the vertical direction, can illuminate the horizontal circulation in the gas vessel separately in three different layers (with lower layer from 0.3–0.9 cm, middle layer from 2.0–2.6 cm, and upper layer from 3.3–3.9 cm) for photography. The vertical light sheet is used to display the flow field structure of the horizontal circulation in its vertical sections, as shown in Fig. 2.

Inside the gas vessel, along its radial lines, there are several small thermal sensors (1 mm in diameter), which are used to measure temperature distributions of the flow field in the horizontal direction of a section at some predefined height. In Fig. 3 temperature curves of a single typhoon, in a section with the height of 3.8 cm equivalent to the height of 15 km (upper layer) of an actual typhoon, are shown. They show similar temperature distributions.

C. Main parameters of experiments

In rotating annulus experiments the values of main parameters would have to satisfy these criteria of dynamic similarity, geometric similarity, and similarity of boundary condition, the variation range of parameters as shown in Table II. Note that it is mainly dependent on H_0, D, and G, of course, also relevant with other criteria. So, it is not easy carrying this kind of experiment, especially using the gas as experimental medium.

TABLE II. The variation range of main parameters in experiments.

Parameter	U_e (cm/s)	L_e (cm)	H_{0e} (cm)	t_e (s)	P_{bulb} (W)
Range of values	2–3	30–40	3–3.9	180–225, 120–150	10–12

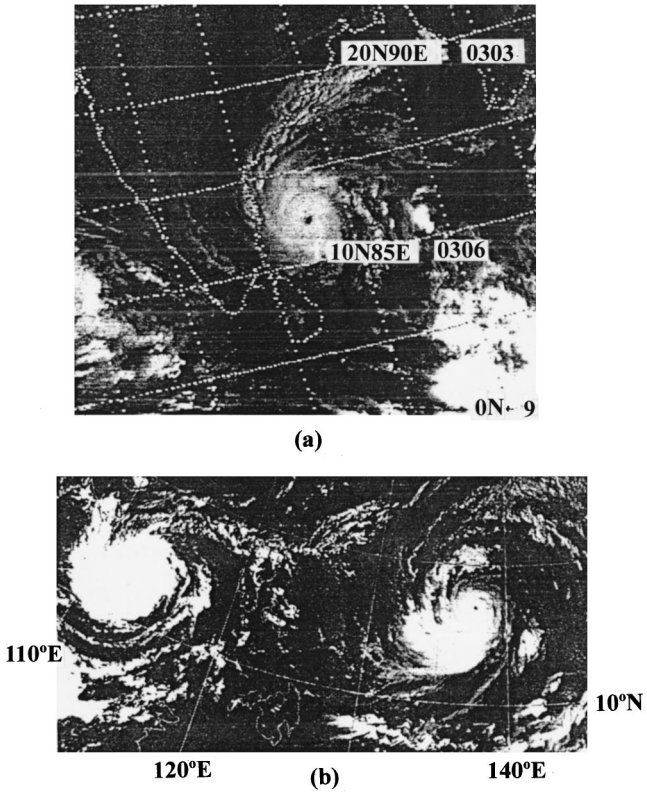

FIG. 4. Satellite photographs. (a) A single typhoon; (b) two typhoons close to each other.

IV. EXPERIMENTAL RESULTS

A. Method of experiment

Two infrared heaters located in the x axis are separated by a distance $l>2r_0$, where r_0 is the maximum radius of a single typhoon. Some amount of smoke is carefully injected into gas vessel while at the same time the annulus starts to rotate with a predefined speed. During this process, the infrared radiation energy was absorbed by the smoke, in turn, the surrounding air was heated by the smoke. A large-scale helical (or vortex) structure began to take its shape gradually. As a consequence, the model typhoon appeared having three different regions, among them the central region was the eye of the typhoon where the air went down. The region surrounding the eye was a strong upward cyclone circulation and the outmost region was a place for an anticyclone circulation and helical cloud bands. It can be seen that the flow structure and its dynamic characteristics of the model typhoon were the same as those of the natural typhoons that one may see in satellite cloud photographs (Fig. 4). As the next step of the experiment, the two model typhoons were allowed to develop into the mature stage, and then the two infrared heaters are moved along x axis. As a result, the outmost regions of the two model typhoons got closer to each other. Then at a certain stage, the infrared heater at the left side was removed [Fig. 5(9)] while the left typhoon continued moving rightwards at the drifting speed. As soon as $l\leqslant r_0/2$, the other infrared heater, i.e., the one on the right side, also ceases working [Fig. 5(13)] and the right typhoon continued moving leftwards at the drifting speed [6] (in large-scale, low-frequency atmospheric flow the drifting speed has an effect on the stability of vortex; see, e.g., [19]). The whole process is similar to typhoons in nature, which keep moving along their original path under the action of environmental air streams or offset forces due to the Coriolis effect. Finally, the two typhoons will collide with each other.

It must be pointed out that for one-dimensional or two-dimensional solitons with a simple structure, one may set different traveling wave speeds in X direction to realize the mutual collision of two solitons in a numerical simulation. However, this method will not work for typhoons with very complicated structures and dynamic processes. The method used in our experiments can make two model typhoons drift with relatively different speeds and, therefore, make them interact with each other without an external source. It is proved to be effective.

B. Collision of model typhoons

Figure 5 shows 32 pictures taken in the laboratory, which are able to demonstrate the whole process of the collision between two model typhoons at various stages (among 32 pictures we take the first one in Fig. 5 as the starting time in a process).

Figure 5(1) shows two model typhoons. They are almost of the same size in their scale. The convergence of vortices and cloud bands of different helical structures are clearly shown. Together with an anticyclone motion outside the typhoons, which can hardly be made out in the pictures due to very weak smoke traces (and which would also agree with the anticyclone motion for typhoons in the Southern Hemisphere), Figs. 5(2)–5(6) show the process when the two typhoons approach each other along the x axis. Their interaction begins when the distance l between the two typhoons is equal to about $2.2r_0$, and the helical cloud bands outside of the typhoons start to combine with each other [Fig. 5(7)]. The interaction becomes more and more intensified when l is getting smaller, as shown in Figs. 5(8)–5(13). When l becomes equal to or slightly less than $1.1r_0$, the two typhoons start rotating around each other, and finally merge into one with their eyes getting obscure as shown in Figs. 5(11)–5(13). After that, their profile assumes an elliptic shape, which is so-called autospinning of typhoons [20], as shown in Figs. 5(14)–5(16). When l approaches zero, the eyes of the two typhoons merge completely into one, which becomes the only identifiable eye one may see inside the combined vortex, but keeps its cyclone motion, as shown in Figs. 5(17)–5(19). Gradually, a separation process starts to show itself at first, the overall shape remains to be as a merged one, with the two inside typhoons rotating around each other: then one sees two eyes showing themselves from the merged typhoon [Figs. 5(20)–5(22)]. After that, the merged typhoon begins to separate [Figs. 5(23)–5(26)], and the respective helical structures of two typhoons are recovered [Figs. 5(27)–5(29)]. One can clearly see the helical cloud bands and cyclone motions of two respective typhoons in the regions outside of their eyes.

After that two typhoons moving along x axis on opposite directions are completely separated as shown in Figs. 5(30)–

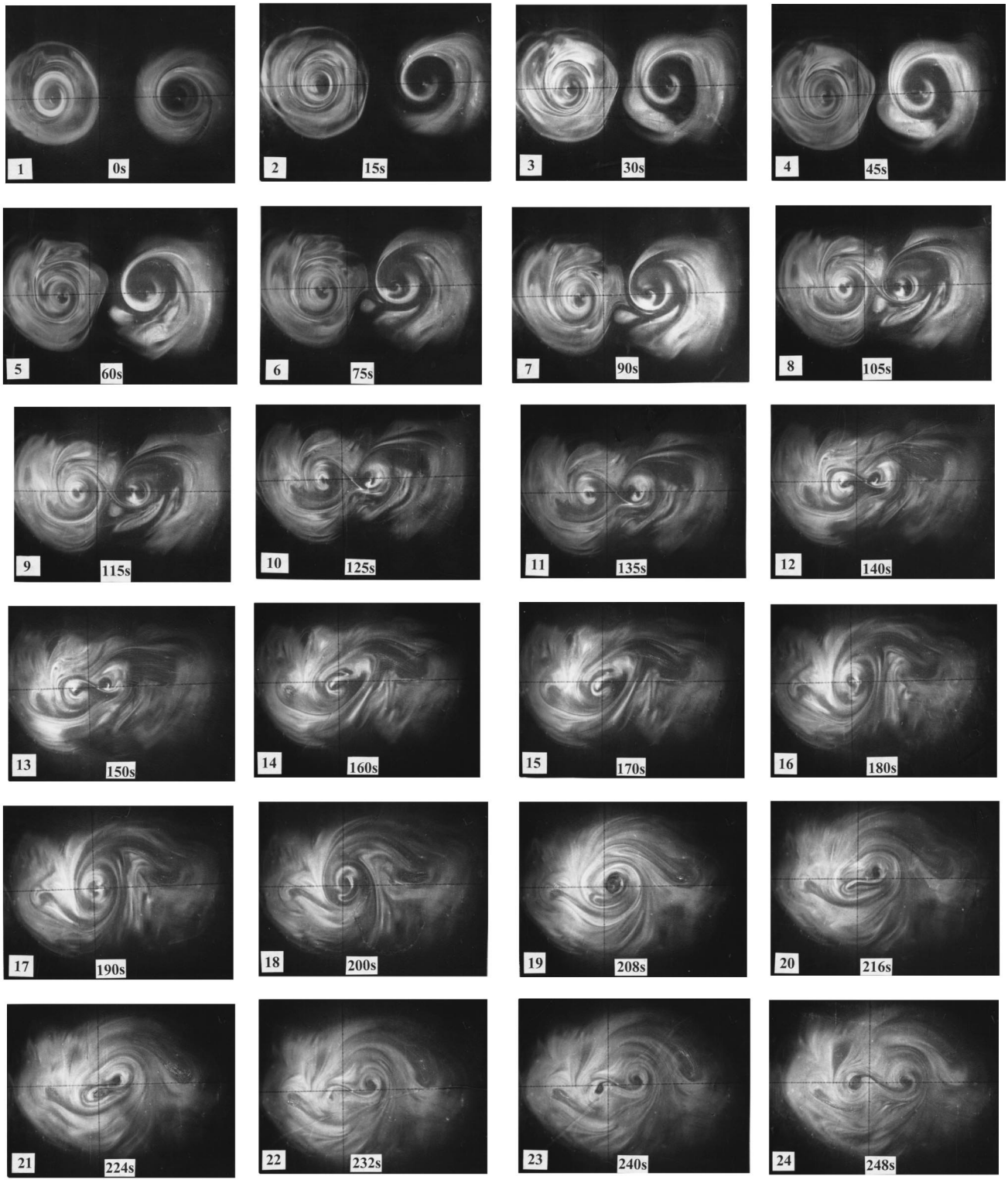

FIG. 5. Laboratory experiment of the collision between two model typhoons.

5(32). Those are the main results of our experiment. Each experiment takes a lot of effort and the success of each experiment hinges on a number of factors, such as the amount of smoke to be injected, the duration of heating, and the speed of movement of the two infrared light sources. The left side heater was removed when the two model typhoons come near to $(0.8-1.0)r_0$ apart as measured by their center distance l (pictures 11–13 in Fig. 5); and the right side heater was removed when $l \leqslant r_0/2$ (pictures 4–16 in Fig. 5). Then the interaction of the two model typhoons took place without any external heat sources. The left model typhoon may drift about a distance of $(0.9-1.1)r_0$. If they are not driven to the

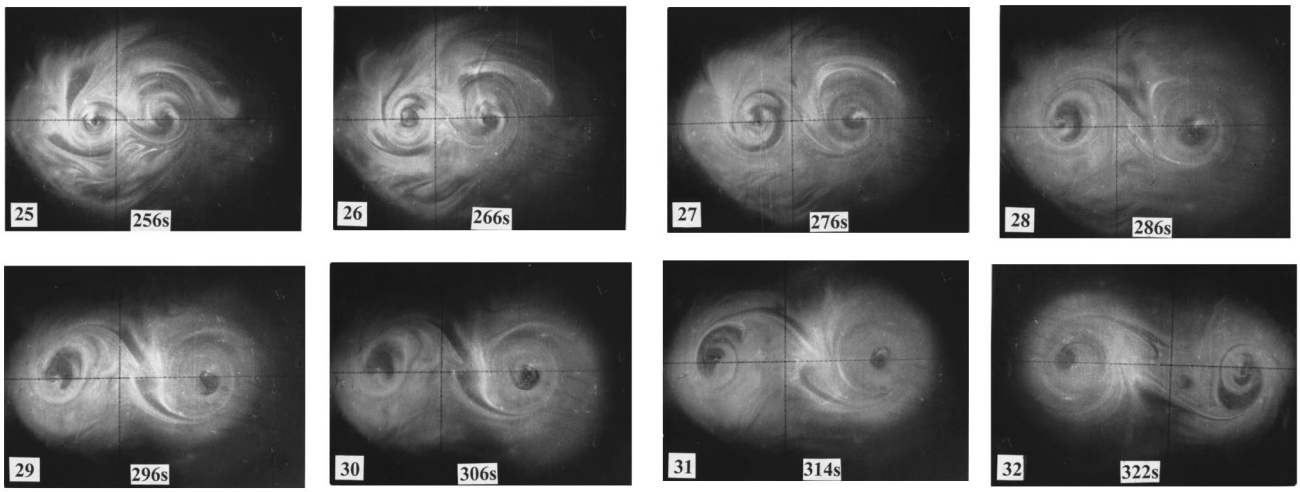

FIG. 5. (*Continued*).

distance of $l \leqslant r_0/2$, their latent heat accumulated may not be enough to sustain their drifting while keeping their helical structures.

Actually the KdV soliton, the Rossby soliton, or the actual typhoon in nature continue accumulating energy after their formation to sustain their soliton profiles. It is indeed very difficult in the experiment to realize the instructions only by the drifting movement of model typhoons.

C. Brief explanation of experiments

From Table I we know that all the similarity parameters, with the exception of Prandtl number Pr, cannot be varied independent of each other, for example, when varying the characteristic length l of a model typhoon, the six parameters will be changed at the same time. Similarly, varying Coriolis parameter f will change all these parameters, such as Ro, Ek and H_0. For the sake of illustration we will give a summary explanation of experiments with different ranges of parameters as below.

(1) Varying the rotating speed n (rpm). When $n < (0.5-0.6)$(rpm), the eye of model typhoon cannot be formed; when $n > 3$(rpm), the helical structure of model typhoon differs from normal typhoon and its structure is very instable.

(2) Decreasing the heating electrical power P_{bulb}(W). The proper heating power P_{bulb} is about 12 W, when the P_{bulb} is between 8 and 10 W, the entire time that is needed to form a mature model typhoon will extend to 5–6 disk day from 3 ones. If the P_{bulb} is below 8 W it is very difficult to form a model typhoon.

(3) Varying the size of model typhoon. In collision experiments of two model typhoons, r_1 and r_2 denote their respective radii: When $r_1 \leqslant 2r_2$ or $r_2 \leqslant 2r_1$, they cannot separate from each other after colliding. The maximum radius and minimum radius of model typhoons are about 20 cm and 10 cm, respectively.

(4) Changing the strength of model typhoon. Varying the heating duration of a model typhoon can change their strengths. For example, we start heating one model typhoon two disk days after heating another model typhoon, so that these two typhoons formed in such a way will have different strength. In general, such model typhoons cannot separate after they come into collision with each other.

(5) Varying displacement speed of model typhoon. After their merging, the two typhoons cannot split successfully if their respective drift speeds are very different, for example, one has 0.5 cm/s and another has 1.0 cm/s before colliding with each other. The collision experiment had been repeated 12 times, of which clear separations were observed 7 times.

V. RESULTS AND DISCUSSIONS

The merger of two typhoons after interaction and their rotations around each other [21] have been extensively verified by many satellite cloud photographs [22,23]. However, the process lasts for very short time, which makes it rather difficult to observe it in nature. No satellite photographs have been obtained to show the whole process, which renders even more importance to our experiment. In order to avoid the influence of the background flow field and the terrain, the top and bottom plates of the gas vessel are made of plexiglass. When the two model typhoons start to merge, the two infrared heaters are consecutively removed with a bit interval of time. Our experiments simulate the state of the natural typhoons when Coriolis force, centrifugal force, and the force due to air pressure gradients come to an equilibrium and the rotating atmospheric system is governed by the following equation:

$$\frac{\nu_\lambda^2}{r} + f\nu_\lambda = \frac{1}{\rho}\frac{\partial P}{\partial r}. \tag{9}$$

So the two model typhoons move along their respective original directions with the drifting speeds and are made to collide without external heat sources. Our laboratory experiments show that the separation does happen after a merger of two typhoons and their helical structure and essential shape are restored (for a typhoon its structure is more meaningful than its shape). It means that the typhoon follows the similar

basic dynamic characteristics of solitons. In other words, a typhoon is a large-scale soliton with helical structures.

In fact typhoons in nature do have large-scale helical structures, with a longevity of about 6 days. Usually they are rapidly broken down as soon as they have made a landfall. Some typhoons with longer longevity are also reported, however, such as the Ginger hurricane in Atlantic in 1971, which lasted as long as 1 month, which shows that the helical structure of the typhoons is fairly stable.

Although a typhoon is a dissipative nonlinear dynamic system, it absorbs a large amount of frozen latent heat on the oceanic surface during its formation process to counteract the energy dissipated by the eddy viscosity, which makes it possible for typhoons to maintain a local stable structure.

In summary, a typhoon follows the following three features: (1) Separation and restoration of its original helical structures after collision, (2) relatively long life, (3) a local structure as the result of dispersion, dissipation, and nonlinear actions. These three features strongly suggest that typhoons are large-scale three-dimensional helical solitons in nature. At the same time, it is expected that the concept of soliton will be extended to be able to describe the kind of very complicated natural phenomena such as typhoons.

ACKNOWLEDGMENTS

Helpful discussions with Professor Wang Keren of IM, Professor Wei Dingwen and Professor Lu Daren of IAP, Professor Chen Siyu of NSFC, Professor Yan Muling, and Professor Wang Keling of CUST are gratefully acknowledged. This work was supported by National Natural Science Foundation of China under Grant No. 49775256.

[1] H. Riehl, *Climate and Weather in the Tropics* (Academic, London, UK, 1979).
[2] R. A. Anthes, *Tropical Cyclones, Their Evolution, Structure and Effects*, Meteor Monographys. No. 41 (American Meteorological Society, Boston, 1982).
[3] R. Scorer, *Dynamics of Meteorology and Climate* (Wiley, Chichester, 1997).
[4] R. Williams and J. C.-L. Chan, J. Atmos. Sci. **51**, 1065 (1994).
[5] R. Elsberry, WMO/TD-No. 693, 1995, pp. 106–197 (unpublished).
[6] G. Holland, J. Atmos. Sci. **41**, 68 (1984).
[7] K. Emanuel, Annu. Rev. Fluid Mech. **23**, 179 (1991).
[8] G. Flierl, Annu. Rev. Fluid Mech. **19**, 493 (1987).
[9] P. Read, Meteorol. Mag. **117**, 35 (1988).
[10] E. Hopfinger and G. J. F. van Heijst, Annu. Rev. Fluid Mech. **25**, 241 (1993).
[11] P. Malamotte-Rizzoli, Adv. Geophys. **24**, 147 (1982).
[12] B. Hoskins and R. Pearce, *Large-Scale Dynamical Processes in the Atmosphere* (Academic, London, UK, 1983).
[13] M. Makino, T. Kamimura, and T. Taniuti, J. Phys. Soc. Jpn. **50**, 980 (1981).
[14] J. Charney, *Mathematical Problems in the Geophysical Science* (AMS, Boston, 1971), pp. 355–373.
[15] H. L. Kuo, J. Atmos. Sci. **31**, 1232 (1974).
[16] M. Yamasaki, J. Meteorol. Soc. Jpn. **22**, 11 (1977).
[17] Wei Dingwen and C. C. Chang, Sci. Sin., Ser. B (Engl. Ed.) **25**, 881 (1982).
[18] C. C. Chang, Wei Dingwen, and Ho Fuhua, Sci. Sin. **18**, 381 (1975).
[19] G. Swaters, Phys. Fluids **29**, 1419 (1986).
[20] S. Brand, J. Appl. Meteorol. **9**, 433 (1970).
[21] M. Lander and J. Holland, Q. J. R. Meteorol. Soc. **47**, 287 (1993).
[22] R. Sheets, Weather and Forcasting **5**, 76 (1990).
[23] I. Haas and R. Shapiro, in *Meteorological Satellites, Past, Present, and Future*, edited by Scientific and Technical Information Branch, NASA Conf. Publ. 2227 (National Aeronautics and Space Administration, Washington, D.C., 1982), pp. 17–29.